

## Specification for Phase II-E Benchmark

### Study on the impact of changes in the isotopic inventory due to control rod insertions in PWR UO<sub>2</sub> fuel assemblies during irradiation on the end effect

Jens Christian Neuber (AREVA Framatome-ANP GmbH, Germany)

#### 1. Introduction

In Phase II-D the effect of control rod (CR) insertion during irradiation of PWR UO<sub>2</sub> fuel assemblies on the spent fuel composition was studied. It was shown that, due to spectrum hardening, CR insertion results in a change of the spent nuclear fuel (SNF) isotopic inventory; and it was demonstrated that, at given initial enrichment and given burnup, SNF which was exposed to CR insertion during irradiation has a higher reactivity than SNF which has not been exposed to CR insertion.

In Phase II-C the impact of the asymmetry of axial burnup profiles of spent PWR UO<sub>2</sub> fuel assemblies on the end effect was studied. It was shown that the end effect increases with increasing asymmetry.

Since the objective of the Phase II program is to study the impact of axial burnup profiles on the reactivity of spent PWR fuel assembly configurations, it is proposed to combine in a Phase II-E benchmark the asymmetry effect on the end effect with the CR insertion effect on the isotopic inventory as set forth below:

- For a given asymmetry, i.e. for a given axial burnup profile the end effect is studied for different CR insertion depths ranging from 0 cm (no insertion) to full insertion. In total fourteen different CR insertion depths are proposed.
- Since the asymmetry of the axial profiles and the end effect are dependent on the average burnup of the profiles (cf. Phase II-C report) two axial profiles are chosen, one related to an average burnup of 30 MWd/kg U, the other related to an average burnup of 50 MWd/kg U.
- To be representative and bounding the axial burnup profiles chosen are generated from a database of real axial burnup profiles by means of the methods described in Reference /1/.

The two axial burnup profiles (in form of two step distributions) are provided for contributors to the Phase II-E benchmark exercise. In addition, the sets of isotopic number densities related to the axial burnup profiles and the different CR insertion depths are provided for contributors to the benchmark exercise. To enable the contributors to estimate the end effects related to the axial profiles and the different insertion depths, the number densities applying to the average burnup values of 30 MWd/kg U and 50 MWd/kg U, respectively, and to the different CR insertion depths are delivered to the contributors.

So, the objective of the Phase II-E benchmark is to study the impact of changes in the spent fuel isotopic composition due to CR insertion on the end effect. For this purpose basically the

same conceptual cask configuration is employed as was already used in the Phase II-B and Phase II-C benchmark exercises.

The Phase II-E benchmark exercise consists of the following sets of calculations:

- Determination of the neutron multiplication factor  $k_{\text{eff}}$  of the cask configuration for the two axial burnup profiles and at least eight different CR insertion depths (cf. Table 3.1, p. 21).
- Determination of the neutron multiplication factor  $k_{\text{eff}}$  of the cask configuration for the uniform distributions of the average burnup values of 30 MWd/kg U and 50 MWd/kg U and for the eight insertion depths.

Optionally, to facilitate more detailed analysis of the effects under study, contributors to Phase II-E are invited to provide the axial fission density distributions for the calculation tasks specified above.

## **2. Problem specification of the Phase II-E benchmark**

### **2.1. Description of the cask configuration to be analyzed**

Basically the same conceptual cask configuration as was already used in the Phase II-B and Phase II-C benchmark exercises is employed in the Phase II-E benchmark. The cask is assumed to be loaded with PWR fuel assemblies of the 17\*17-(24+1) type, cf. Figure 2.1. As illustrated in Figures 2.3 and 2.4, twenty-one fuel assemblies of this type are positioned in a borated stainless steel basket centered in the transport cask which is assumed to be fully flooded.

#### **2.1.1. Fuel assembly data**

- Fuel rod:
  - Spent fuel material: see sections 2.2.2 and 2.2.3
  - Fuel diameter: 0.8166 cm
  - Cladding inner diameter (= Gap diameter): 0.833 cm
  - Cladding outer diameter: 0.955 cm
  - Cladding material: Zircaloy (number densities given in Table 2.1)
  - Active length: 365.76 cm
  - Full length: 386.71
  - Location of the active zone within the fuel rod: Central positioning within the fuel rod (cf. Figures 2.2 and 2.4; the active zone is colored in red in these figures)
  - The zones between the ends of the active zone and the ends of the fuel rods (colored in green in Figures 2.2 and 2.4): These zones consist of cladding with vacuum (void) inside and water outside; springs and plugs are to be ignored.

- Guide thimble and instrumentation tube:
  - Inner diameter: 1.138 cm
  - Outer diameter: 1.224 cm
  - Length: 386.71 cm
  - Material: Zircaloy (cf. Table 2.1)

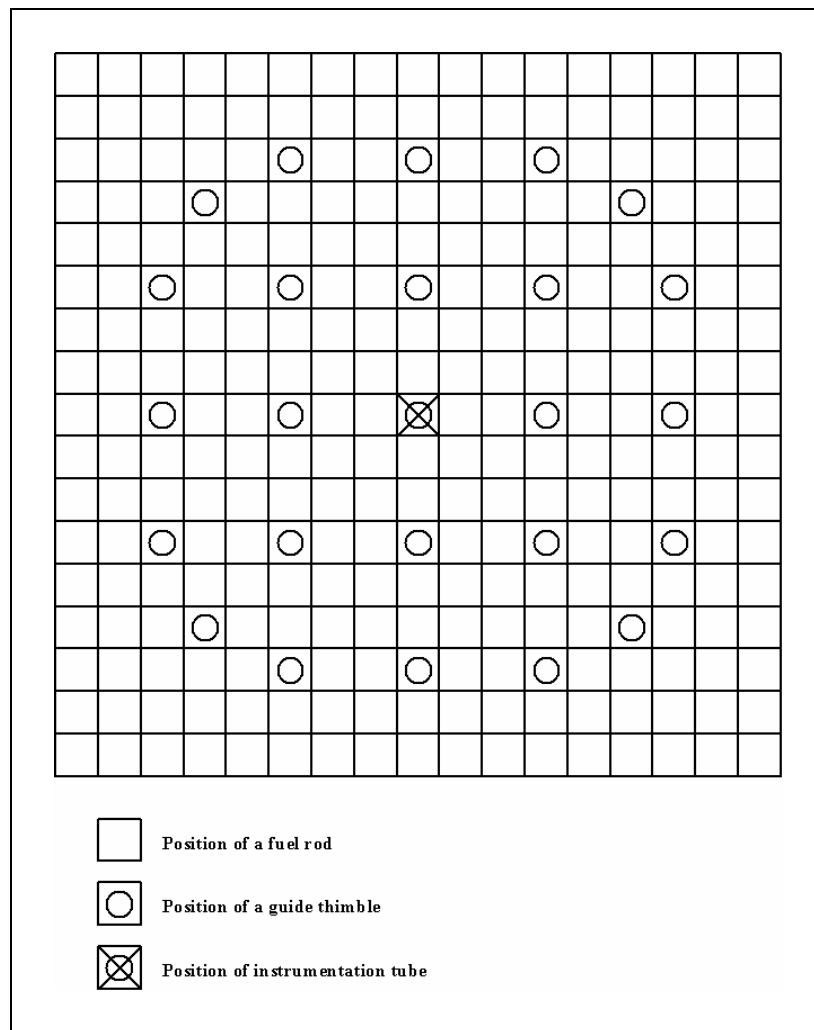


**Figure 2.1: 17x17-(24-1) fuel assembly lattice type**

- Lattice (cf. Figure 2.1):
  - 17x17 lattice type
  - Number of fuel rods: 264
  - Number of guide thimbles: 24 (cf. Table 2.1)
  - Number of instrumentation tubes: 1 (cf. Table 2.1)
  - Rod pitch: 1.26 cm
  - Spacer grids: To be ignored

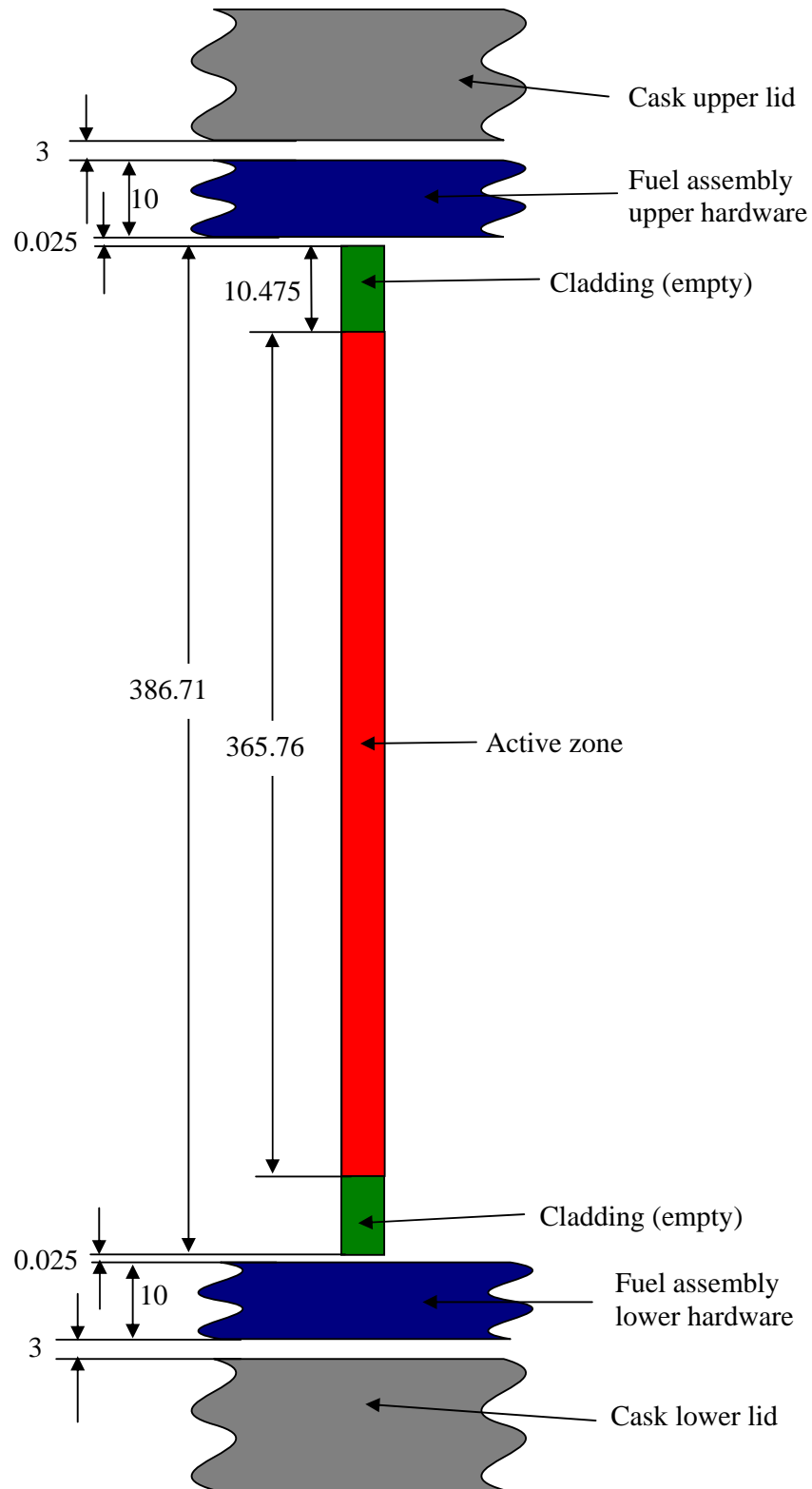


Figure 2.2: Fuel rod (schematic)

(Dimension in cm)

- Fuel assembly lower and upper hardware (cf. Figures 2.2 and 2.4):
  - Geometric cross section: 21.42x21.42 cm<sup>2</sup>
  - Length: 10 cm

The lower and the upper hardware zones of the fuel assemblies are colored in blue in Figures 2.2 and 2.4. These zones are assumed to be regions of smeared stainless steel (50 Vol.-%) and water (50 Vol.-%). The atomic number densities are given in Table 2.1.

As follows from the fuel assembly data specified above, the fuel assembly assumed is not quite realistic. The central positioning of the active fuel zone with respect to top and bottom ends of the fuel rods, the same size for the lower and upper fuel hardware, the same distance for the bottom end of the lower hardware from the lower cask lid and the top end of the upper hardware from the upper cask lid, and the same size for the lower and upper cask lid are assumed in order to have identical neutron reflection conditions at bottom and top end of the fuel zone (cf. Phase II-C report).

**Table 2.1: Atomic number density (in b<sup>-1</sup>cm<sup>-1</sup>) of structural materials and water**

Cladding material, guide thimble and instrumentation tube material	Zircaloy	Cr	7.589E-05
		Fe	1.484E-04
		Zr	4.298E-02
Fuel assembly hardware	50%/50% stainless steel / water mixture	Cr	8.714E-03
		Mn	8.682E-04
		Fe	2.968E-02
		Ni	3.860E-03
		H	3.337E-02
		O	1.669E-02
Basket material	Borated (1 wt.-%) stainless steel	Cr	1.691E-02
		Mn	1.684E-03
		Fe	5.758E-02
		Ni	7.489E-03
		B-10	7.836E-04
		B-11	3.181E-03
Cask material	Stainless steel	Cr	1.743E-02
		Mn	1.736E-03
		Fe	5.936E-02
		Ni	7.721E-03
Water		H	6.675E-02
		O	3.337E-02

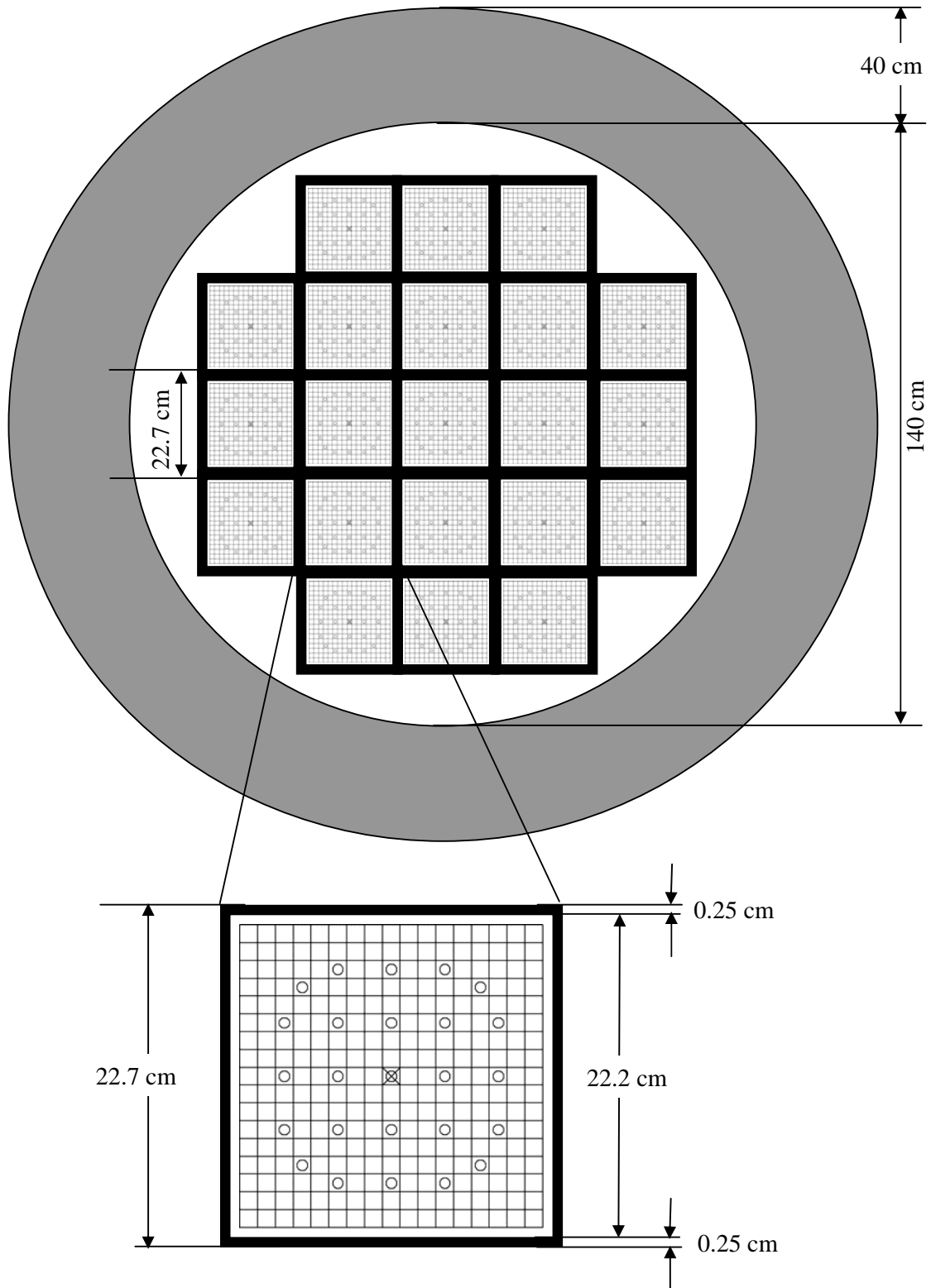


Figure 2.3: Phase II-E cask configuration: top view of the cask (at axial midplane)

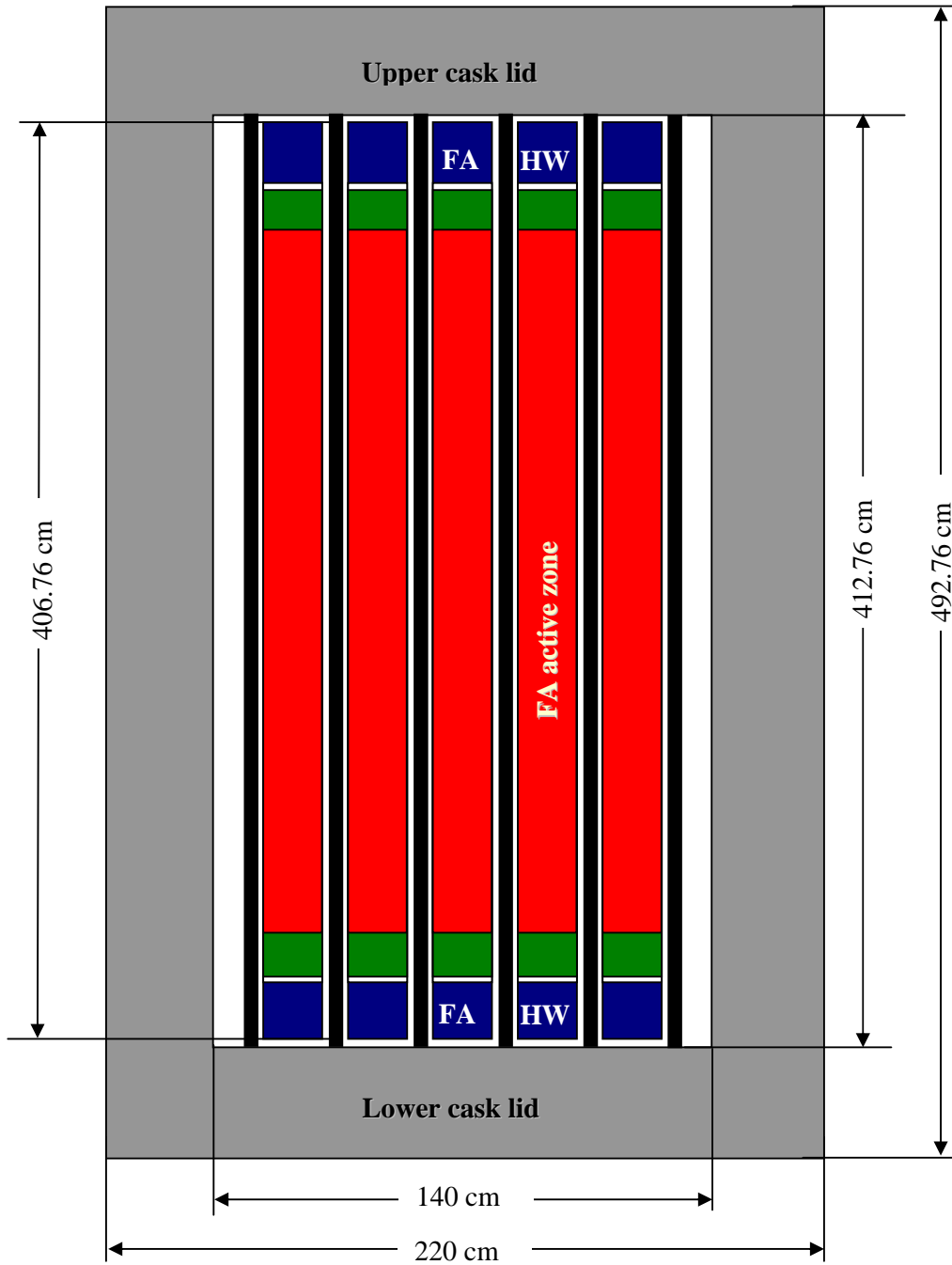


Figure 2.4: Phase II-E cask configuration: side view of the cask  
(FAHW:= fuel assembly hardware)

### 2.1.2. Fuel assembly basket

- Inner basket compartment dimensions:  $22.2 \times 22.2 \times 412.76 \text{ cm}^3$  (each fuel assembly position, cf. Figures 2.3 and 2.4)
- Basket wall thickness: 0.25 cm (everywhere; only one basket wall between two adjacent fuel assembly positions, cf. Figures 2.3 and 2.4)
- Basket material: Borated stainless steel with 1 wt.-% of natural boron (atomic number densities given in Table 2.1)

(The basket material is presented in black color in Figures 2.3 and 2.4.)

### 2.1.3. Cask

- Cask shell (cf. Figures 2.3 and 2.4):
  - Inner diameter: 140 cm
  - Outer diameter: 220 cm
  - Height:
    - Inner cavity: 412.76 cm
    - Outside: 492.76 cm
  - Material: Stainless steel (atomic number densities given in Table 2.1)

(The cask material is presented in grey in Figures 2.2 through 2.4.)

### 2.1.4. Configuration

- 21 fuel assemblies in a 5x5 array (without corner positions) as shown in Figure 2.3
- Fuel assemblies placed centrally within the basket compartments (cf. Figure 2.4)
- Cask completely flooded with water (atomic number densities of water given in Table 2.1).

(Don't forget: There is a water gap between the lower fuel assembly hardware and the lower cask lid in order to have identical neutron reflection conditions at bottom and top end of the fuel zone, cf. Figures 2.2 and 2.4.)

## 2.2. Axial burnup profiles and control rod insertion depths

### 2.2.1. Axial zoning of the profiles and control rod insertion depths

The bounding axial burnup profiles selected for the Phase II-E benchmark are presented in Figure 2.5. These profiles were obtained from a 17x17-(24-1) PWR UO<sub>2</sub> assembly type axial burnup profile database by means of the methods described in Ref. /1/.

As indicated in Figure 2.5 the profiles are given on 35 nodes. As is obvious from this figure, due to the shape of the profiles it is reasonable to group some of the nodes in a few axial zones together. As given in Table 2.2, the Phase II-E axial burnup model distributions are thus defined by 19 axial zones. However, as specified in Tables 2.3 through 2.16, due to the CR insertion depth it is necessary in some of the Phase II-E benchmark cases to split one of the axial zones in two zones and use 20 axial zones in these instances. <sup>1)</sup>

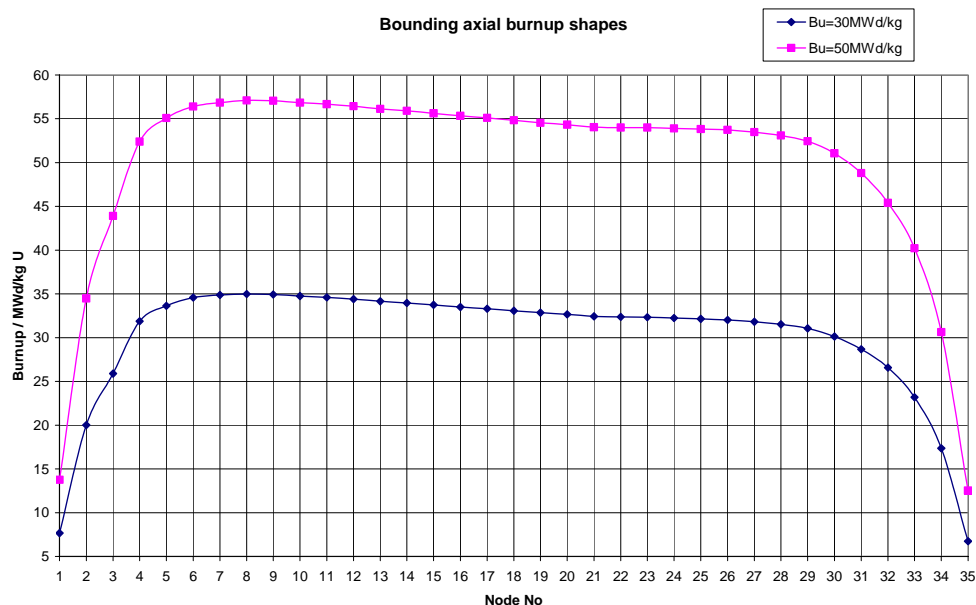


**Figure 2.5: The bounding axial burnup profiles selected for the Phase II-E benchmark**

### 2.2.2. Isotopic number densities for the axial zones of the profiles

The isotopic number densities for the axial zones of the profiles are given in ASCII II formatted files named as “edxx\_f01\_idnnnnn\_bmm.mip”. “idnnnnn” in this names is the indicator of the related CR insertion depth (“id01045” stands for the insertion depth 10.45 cm for instance); and “bmm” is the indicator of the average burnup value of the profiles (“b30” stands for 30 MWd/kg U average burnup for instance). (The indicators “edxx” and “f01” of the file names are of no importance for contributors to the benchmark).

The names of these files are specified in Tables 2.3 through 2.16. The structure of these files is explained in Table 2.17. As indicated in this table, the isotopic number densities are given in the order of the axial zones specified in Tables 2.3 through 2.16. The number densities refer to an initial enrichment of 4 wt.-% and are given in units of  $b^{-1} \cdot cm^{-1}$ .

All the number densities given refer to the fuel diameter specified in section 2.1.1.

<sup>1)</sup> Splitting of one zone in two zones under otherwise unchanged conditions has no physical impact on the neutron multiplication factor  $k_{eff}$  and on the axial fission density distribution. Both parts of the split zone have one and the same burnup. So, if both parts have one and the same isotopic inventory they are identical.

**Table 2.2: Phase II-E axial burnup model distributions**

```

FA-Name: 1001_MEAN---030
lfd.Nr.: 1 average discharge burnup: 3.00000E+01 MWd/kg U

Model distribution: 19 axial zones (delta B = 0.0E+00)
Zone No. Node-Start Node-End upper bound / cm average burnup / MWd/kg
1 1 1 10.45 7.66318E+00
2 2 2 20.90 2.00120E+01
3 3 3 31.35 2.58859E+01
4 4 4 41.80 3.18662E+01
5 5 5 52.25 3.36237E+01
6 6 6 62.70 3.45706E+01
7 7 10 104.50 3.48843E+01
8 11 14 146.30 3.42845E+01
9 15 18 188.11 3.34082E+01
10 19 20 209.01 3.27585E+01
11 21 26 271.71 3.22534E+01
12 27 28 292.61 3.16631E+01
13 29 29 303.06 3.10535E+01
14 30 30 313.51 3.01256E+01
15 31 31 323.96 2.86700E+01
16 32 32 334.41 2.65620E+01
17 33 33 344.86 2.31914E+01
18 34 34 355.31 1.73624E+01
19 35 35 365.76 6.74193E+00
=====

FA-Name: 1002_MEAN---050
lfd.Nr.: 2 average discharge burnup: 5.00000E+01 MWd/kg U

Model distribution: 19 axial zones (delta B = 0.0E+00)
Zone No. Node-Start Node-End upper bound / cm average burnup / MWd/kg
1 1 1 10.45 1.37685E+01
2 2 2 20.90 3.44919E+01
3 3 3 31.35 4.39043E+01
4 4 4 41.80 5.23878E+01
5 5 5 52.25 5.50777E+01
6 6 6 62.70 5.64093E+01
7 7 10 104.50 5.69651E+01
8 11 14 146.30 5.62904E+01
9 15 18 188.11 5.52262E+01
10 19 20 209.01 5.44358E+01
11 21 26 271.71 5.39196E+01
12 27 28 292.61 5.32875E+01
13 29 29 303.06 5.24371E+01
14 30 30 313.51 5.10594E+01
15 31 31 323.96 4.88051E+01
16 32 32 334.41 4.53876E+01
17 33 33 344.86 4.02173E+01
18 34 34 355.31 3.06352E+01
19 35 35 365.76 1.25278E+01
=====

Ende

Uebersicht, geordnet nach average discharge burnup (ADB):

ADB= 30.00000 lfd.Nr.: 1 FA-Name: 1001_MEAN---030
ADB= 50.00000 lfd.Nr.: 2 FA-Name: 1002_MEAN---050

```

**Table 2.3: Axial zoning of the Phase II-E axial burnup model distributions for a CR insertion depth of 0 cm**

Axial zone No	Height of the upper bound of the zone/ cm
1	10.45
2	20.90
3	31.35
4	41.80
5	52.25
6	62.70
7	104.50
8	146.30
9	188.11
10	209.01
11	271.71
12	292.61
13	303.06
14	313.51
15	323.96
16	334.41
17	344.86
18	355.31
19	365.76

-----

Axial burnup model distribution isotopic number densities:  
 - average burnup = 30 MWd/kg U: ed13\_f01\_id00000\_b30.mip  
 - average burnup = 50 MWd/kg U: ed13\_f01\_id00000\_b50.mip

**Table 2.4: Axial zoning of the Phase II-E axial burnup model distributions for a CR insertion depth of 5.22 cm**

Axial zone No	Height of the upper bound of the zone/ cm
1	10.45
2	20.90
3	31.35
4	41.80
5	52.25
6	62.70
7	104.50
8	146.30
9	188.11
10	209.01
11	271.71
12	292.61
13	303.06
14	313.51
15	323.96
16	334.41
17	344.86
18	355.31
19	360.54
20	365.76

-----

Axial burnup model distribution isotopic number densities:  
 - average burnup = 30 MWd/kg U: ed24\_f01\_id00522\_b30.mip  
 - average burnup = 50 MWd/kg U: ed24\_f01\_id00522\_b50.mip

**Table 2.5: Axial zoning of the Phase II-E axial burnup model distributions for a CR insertion depth of 10.45 cm**

Axial zone No	Height of the upper bound of the zone/ cm	
1	10.45	
2	20.90	
3	31.35	
4	41.80	
5	52.25	
6	62.70	
7	104.50	
8	146.30	
9	188.11	
10	209.01	
11	271.71	
12	292.61	
13	303.06	
14	313.51	
15	323.96	
16	334.41	
17	344.86	
18	355.31	
19	365.76	CR

-----

Axial burnup model distribution isotopic number densities:  
 - average burnup = 30 MWd/kg U: ed24\_f01\_id01045\_b30.mip  
 - average burnup = 50 MWd/kg U: ed24\_f01\_id01045\_b50.mip

**Table 2.6: Axial zoning of the Phase II-E axial burnup model distributions for a CR insertion depth of 15.67 cm**

Axial zone No	Height of the upper bound of the zone/ cm	
1	10.45	
2	20.90	
3	31.35	
4	41.80	
5	52.25	
6	62.70	
7	104.50	
8	146.30	
9	188.11	
10	209.01	
11	271.71	
12	292.61	
13	303.06	
14	313.51	
15	323.96	
16	334.41	
17	344.86	
18	350.09	
19	355.31	CR
20	365.76	CR

-----

Axial burnup model distribution isotopic number densities:  
 - average burnup = 30 MWd/kg U: ed24\_f01\_id01567\_b30.mip  
 - average burnup = 50 MWd/kg U: ed24\_f01\_id01567\_b50.mip

**Table 2.7: Axial zoning of the Phase II-E axial burnup model distributions for a CR insertion depth of 20.90 cm**

Axial zone No	Height of the upper bound of the zone/ cm	
1	10.45	
2	20.90	
3	31.35	
4	41.80	
5	52.25	
6	62.70	
7	104.50	
8	146.30	
9	188.11	
10	209.01	
11	271.71	
12	292.61	
13	303.06	
14	313.51	
15	323.96	
16	334.41	
17	344.86	
18	355.31	CR
19	365.76	CR

-----

Axial burnup model distribution isotopic number densities:  
 - average burnup = 30 MWd/kg U: ed24\_f01\_id02090\_b30.mip  
 - average burnup = 50 MWd/kg U: ed24\_f01\_id02090\_b50.mip

**Table 2.8: Axial zoning of the Phase II-E axial burnup model distributions for a CR insertion depth of 26.12 cm**

Axial zone No	Height of the upper bound of the zone/ cm	
1	10.45	
2	20.90	
3	31.35	
4	41.80	
5	52.25	
6	62.70	
7	104.50	
8	146.30	
9	188.11	
10	209.01	
11	271.71	
12	292.61	
13	303.06	
14	313.51	
15	323.96	
16	334.41	
17	339.64	
18	344.86	CR
19	355.31	CR
20	365.76	CR

-----

Axial burnup model distribution isotopic number densities:  
 - average burnup = 30 MWd/kg U: ed24\_f01\_id02612\_b30.mip  
 - average burnup = 50 MWd/kg U: ed24\_f01\_id02612\_b50.mip

**Table 2.9: Axial zoning of the Phase II-E axial burnup model distributions for a CR insertion depth of 31.35 cm**

Axial zone No	Height of the upper bound of the zone/ cm	
1	10.45	
2	20.90	
3	31.35	
4	41.80	
5	52.25	
6	62.70	
7	104.50	
8	146.30	
9	188.11	
10	209.01	
11	271.71	
12	292.61	
13	303.06	
14	313.51	
15	323.96	
16	334.41	
17	344.86	CR
18	355.31	CR
19	365.76	CR

-----

Axial burnup model distribution isotopic number densities:  
- average burnup = 30 MWd/kg U: ed24\_f01\_id03135\_b30.mip  
- average burnup = 50 MWd/kg U: ed24\_f01\_id03135\_b50.mip

**Table 2.10: Axial zoning of the Phase II-E axial burnup model distributions for a CR insertion depth of 36.57 cm**

Axial zone No	Height of the upper bound of the zone/ cm	
1	10.45	
2	20.90	
3	31.35	
4	41.80	
5	52.25	
6	62.70	
7	104.50	
8	146.30	
9	188.11	
10	209.01	
11	271.71	
12	292.61	
13	303.06	
14	313.51	
15	323.96	
16	329.19	
17	334.41	CR
18	344.86	CR
19	355.31	CR
20	365.76	CR

-----

Axial burnup model distribution isotopic number densities:  
- average burnup = 30 MWd/kg U: ed24\_f01\_id03657\_b30.mip  
- average burnup = 50 MWd/kg U: ed24\_f01\_id03657\_b50.mip

**Table 2.11: Axial zoning of the Phase II-E axial burnup model distributions for a CR insertion depth of 41.80 cm**

Axial zone No	Height of the upper bound of the zone/ cm	
1	10.45	
2	20.90	
3	31.35	
4	41.80	
5	52.25	
6	62.70	
7	104.50	
8	146.30	
9	188.11	
10	209.01	
11	271.71	
12	292.61	
13	303.06	
14	313.51	
15	323.96	
16	334.41	CR
17	344.86	CR
18	355.31	CR
19	365.76	CR

-----

Axial burnup model distribution isotopic number densities:  
 - average burnup = 30 MWd/kg U: ed24\_f01\_id04180\_b30.mip  
 - average burnup = 50 MWd/kg U: ed24\_f01\_id04180\_b50.mip

**Table 2.12: Axial zoning of the Phase II-E axial burnup model distributions for a CR insertion depth of 52.25 cm**

Axial zone No	Height of the upper bound of the zone/ cm	
1	10.45	
2	20.90	
3	31.35	
4	41.80	
5	52.25	
6	62.70	
7	104.50	
8	146.30	
9	188.11	
10	209.01	
11	271.71	
12	292.61	
13	303.06	
14	313.51	
15	323.96	CR
16	334.41	CR
17	344.86	CR
18	355.31	CR
19	365.76	CR

-----

Axial burnup model distribution isotopic number densities:  
 - average burnup = 30 MWd/kg U: ed24\_f01\_id05225\_b30.mip  
 - average burnup = 50 MWd/kg U: ed24\_f01\_id05225\_b50.mip

**Table 2.13: Axial zoning of the Phase II-E axial burnup model distributions for a CR insertion depth of 62.70 cm**

Axial zone No	Height of the upper bound of the zone/ cm	
1	10.45	
2	20.90	
3	31.35	
4	41.80	
5	52.25	
6	62.70	
7	104.50	
8	146.30	
9	188.11	
10	209.01	
11	271.71	
12	292.61	
13	303.06	
14	313.51	CR
15	323.96	CR
16	334.41	CR
17	344.86	CR
18	355.31	CR
19	365.76	CR

-----

Axial burnup model distribution isotopic number densities:  
- average burnup = 30 MWd/kg U: ed24\_f01\_id06270\_b30.mip  
- average burnup = 50 MWd/kg U: ed24\_f01\_id06270\_b50.mip

**Table 2.14: Axial zoning of the Phase II-E axial burnup model distributions for a CR insertion depth of 73.15 cm**

Axial zone No	Height of the upper bound of the zone/ cm	
1	10.45	
2	20.90	
3	31.35	
4	41.80	
5	52.25	
6	62.70	
7	104.50	
8	146.30	
9	188.11	
10	209.01	
11	271.71	
12	292.61	
13	303.06	CR
14	313.51	CR
15	323.96	CR
16	334.41	CR
17	344.86	CR
18	355.31	CR
19	365.76	CR

-----

Axial burnup model distribution isotopic number densities:  
- average burnup = 30 MWd/kg U: ed24\_f01\_id07315\_b30.mip  
- average burnup = 50 MWd/kg U: ed24\_f01\_id07315\_b50.mip

**Table 2.15: Axial zoning of the Phase II-E axial burnup model distributions for a CR insertion depth of 94.05 cm**

Axial zone No	Height of the upper bound of the zone/ cm	
1	10.45	
2	20.90	
3	31.35	
4	41.80	
5	52.25	
6	62.70	
7	104.50	
8	146.30	
9	188.11	
10	209.01	
11	271.71	
12	292.61	CR
13	303.06	CR
14	313.51	CR
15	323.96	CR
16	334.41	CR
17	344.86	CR
18	355.31	CR
19	365.76	CR

-----

Axial burnup model distribution isotopic number densities:  
 - average burnup = 30 MWd/kg U: ed24\_f01\_id09405\_b30.mip  
 - average burnup = 50 MWd/kg U: ed24\_f01\_id09405\_b50.mip

**Table 2.16: Axial zoning of the Phase II-E axial burnup model distributions for a CR insertion depth of 365.76 cm**

Axial zone No	Height of the upper bound of the zone/ cm	
1	10.45	CR
2	20.90	CR
3	31.35	CR
4	41.80	CR
5	52.25	CR
6	62.70	CR
7	104.50	CR
8	146.30	CR
9	188.11	CR
10	209.01	CR
11	271.71	CR
12	292.61	CR
13	303.06	CR
14	313.51	CR
15	323.96	CR
16	334.41	CR
17	344.86	CR
18	355.31	CR
19	365.76	CR

-----

Axial burnup model distribution isotopic number densities:  
 - average burnup = 30 MWd/kg U: ed24\_f01\_id36576\_b30.mip  
 - average burnup = 50 MWd/kg U: ed24\_f01\_id36576\_b50.mip



**Table 2.18: Structure of the isotopic inventory files for the uniform axial profiles**

```

BUNUSP Version 7                                     17.05.2005 14:25:51
edl3_f01.sca: siehe Page 1 in Protokollfile edl3_f01.PRT
ffffffffffffffffffffffffffffffffffffffffffffffffffffffffffffffffffffffffffff

Fuel No. 1
enrich.: 4.000E+00 wt.-% burnup: 3.00000E+01 Mwd/kg U                               SCALE

mo-95      1      0.0  3.43000E-05  293.0  end
tc-99      1      0.0  4.04760E-05  293.0  end
ru-101     1      0.0  3.83190E-05  293.0  end
rh-103     1      0.0  2.03460E-05  293.0  end
ag-109     1      0.0  2.70110E-06  293.0  end
cs-133     1      0.0  4.19200E-05  293.0  end
nd-143     1      0.0  3.04210E-05  293.0  end
nd-145     1      0.0  2.43640E-05  293.0  end
sm-147     1      0.0  2.17010E-06  293.0  end
sm-149     1      0.0  1.04440E-07  293.0  end
sm-150     1      0.0  9.54670E-06  293.0  end
sm-151     1      0.0  5.17350E-07  293.0  end
sm-152     1      0.0  4.04410E-06  293.0  end
eu-153     1      0.0  3.46580E-06  293.0  end
gd-155     1      0.0  1.07780E-09  293.0  end
u-234      1      0.0  5.14820E-06  293.0  end
u-235      1      0.0  3.50970E-04  293.0  end
u-236      1      0.0  1.01040E-04  293.0  end
u-238      1      0.0  2.15690E-02  293.0  end
np-237     1      0.0  8.27450E-06  293.0  end
pu-238     1      0.0  2.10600E-06  293.0  end
pu-239     1      0.0  1.31020E-04  293.0  end
pu-240     1      0.0  3.96790E-05  293.0  end
pu-241     1      0.0  2.47510E-05  293.0  end
pu-242     1      0.0  6.18580E-06  293.0  end
am-241     1      0.0  6.00040E-07  293.0  end
am-243     1      0.0  8.76520E-07  293.0  end
o          1      0.0  4.58960E-02  293.0  end
mo-95      2      0.0  3.34980E-05  293.0  end
tc-99      2      0.0  3.97470E-05  293.0  end
ru-101     2      0.0  3.83070E-05  293.0  end
rh-103     2      0.0  2.09740E-05  293.0  end
ag-109     2      0.0  2.93870E-06  293.0  end
cs-133     2      0.0  4.09630E-05  293.0  end
nd-143     2      0.0  3.10060E-05  293.0  end
nd-145     2      0.0  2.38280E-05  293.0  end
sm-147     2      0.0  1.95960E-06  293.0  end
sm-149     2      0.0  1.57440E-07  293.0  end
sm-150     2      0.0  9.70630E-06  293.0  end
sm-151     2      0.0  7.25800E-07  293.0  end
sm-152     2      0.0  3.83620E-06  293.0  end
eu-153     2      0.0  3.64670E-06  293.0  end
gd-155     2      0.0  1.88530E-09  293.0  end
u-234      2      0.0  4.83660E-06  293.0  end
u-235      2      0.0  3.87710E-04  293.0  end
u-236      2      0.0  1.00940E-04  293.0  end
u-238      2      0.0  2.14660E-02  293.0  end
np-237     2      0.0  1.03170E-05  293.0  end
pu-238     2      0.0  2.87830E-06  293.0  end
pu-239     2      0.0  1.84910E-04  293.0  end
pu-240     2      0.0  4.45280E-05  293.0  end
pu-241     2      0.0  3.20040E-05  293.0  end
pu-242     2      0.0  6.45830E-06  293.0  end
am-241     2      0.0  8.02050E-07  293.0  end
am-243     2      0.0  1.11220E-06  293.0  end
o          2      0.0  4.58960E-02  293.0  end
ffffffffffffffffffffffffffffffffffffffffffffffffffffffffffffffffffffffffffff
Ende des Files unifo_cr_part_b30.mip

```

not exposed to CR insertion

exposed to CR insertion

### 2.2.3. Uniform axial burnup distributions

The isotopic number densities for the uniform axial burnup distributions are given in the files

- unifo\_cr\_out\_b30.mip and unifo\_cr\_out\_b50.mip for the case of no CR insertion (CR insertion depth 0cm)
- unifo\_cr\_part\_b30.mip and unifo\_cr\_part\_b50.mip for the case of partial CR insertion (CR insertion depths ranging from 5.22 cm to 94.05 cm, cf. Tables 2.4 through 2.15)
- unifo\_cr\_full\_b30.mip and unifo\_cr\_full\_b50.mip for the case of full CR insertion (CR insertion depth 365.76 cm).

An example for these files is given in Table 2.18. As indicated in this table, the “axial zone number 1” is now the part of the fuel which has not been exposed to CR insertion, the “axial zone number 2” is the part of the fuel which has been exposed to CR insertion.

Note:

- Do not mix the densities of “axial zone number 1” and “axial zone number 2” by any weighting procedure (e.g., weighting according to the CR insertion depth). It is not the objective of the Phase II-E benchmark to assess such weighting procedures.
- If one wants to contribute to the estimation of axial fission density distributions one has to apply the axial zoning specified in Tables 2.3 through 2.16 to the uniform distributions too.
- All the number densities given refer to the fuel diameter specified in section 2.1.1.

## 3. Calculation tasks

### 3.1. Specification of the calculation tasks

- **Task 1:** Reactivity calculations with the two bounding axial burnup profiles (cf. section 2.2.1): Determination of the neutron multiplication factors  $k_{\text{eff}}$  of the above-specified Phase II-E cask configuration for at least eight CR insertion depths as summarized in Table 3.1. As given in this table, it is recommended to consider the CR insertion depths 0 cm (no insertion), 10.45 cm, 20.90 cm, 31.35 cm, 41.80 cm, 52.25 cm, 73.15 cm, and 365.76 cm (full insertion). (Axial zoning and number densities: see sections 2.2.1 and 2.2.2.)
- **Task 2:** Reactivity calculations with the uniform distributions of the average burnup values of 30 MWd/kg U and 50 MWd/kg : Determination of the neutron multiplication factors  $k_{\text{eff}}$  of the Phase II-E cask configuration for the CR insertion depths selected in task No. 1. (Number densities: see section 2.2.3)
- **Task 3 (optional):** Together with task No. 1 fission density calculations with the two bounding axial burnup profiles: Determination of the fission densities in the axial zones specified in Tables 2.3 through 2.16. Fission densities as defined in Phase II-A and Phase II-C:

**Table 3.1: Summary of CR insertion depths to be considered**

CR insertion depth / cm	Axial zoning	Remark
0.0	Table 2.3	
5.22	Table 2.4	<b>optional</b>
10.45	Table 2.5	
15.67	Table 2.6	<b>optional</b>
20.90	Table 2.7	
26.12	Table 2.8	<b>optional</b>
31.35	Table 2.9	
36.57	Table 2.10	<b>optional</b>
41.80	Table 2.11	
52.25	Table 2.12	
62.70	Table 2.13	<b>optional</b>
73.15	Table 2.14	
94.05	Table 2.15	<b>optional</b>
365.76	Table 2.16	

$$\rho_i = \frac{\frac{1}{V_i} \int_{V_i} \Sigma_f(\vec{r}, E) \Phi(\vec{r}, E) d\vec{r} dE}{\sum_{j=1}^m \frac{1}{V_j} \int_{V_j} \Sigma_f(\vec{r}, E) \Phi(\vec{r}, E) d\vec{r} dE}, \quad i = 1, \dots, m, \quad (m = 19 \text{ or } m = 20) \quad (3.1)$$

$\Phi(\vec{r}, E) :=$  flux at locus  $\vec{r}$  and energy  $E$ ,

$\Sigma_f(\vec{r}, E) :=$  macroscopic fission cross section at  $\vec{r}$  and  $E$ ,

$V_i :=$  volume of the  $i$ -th axial zone,  $i = 1, \dots, m$ .

- **Task 4 (optional):** Together with task No. 2 fission density calculations with the uniform burnup distributions: Determination of the fission densities in the axial zones specified in Tables 2.3 through 2.16. Fission densities as defined by eq.(3.1).

Note:

- The recorded fission densities must be different from zero for each axial zone (cf. Ref. /2/) if the test procedure described in section 3.2 is used.
- Convergence in the calculation of the axial fission density distributions shall be checked.
  - It is therefore recommended to figure out the minimum required number of initial neutron generations to be skipped in the evaluation of the individual calculation runs by means of the statistical test procedure described in section 3.2.
  - Note that this test procedure requires the use of different starting random numbers for each of the calculation runs evaluated by the test procedure.

- Remark: It is not necessary to perform a convergence test for each of the individual cases specified in Table 3.1 for the non-uniform axial burnup profiles (task No.3) and the uniform burnup distribution (task No.4). It is sufficient to apply this test to a representative and crucial case. Such a case is certainly given when a non-uniform axial burnup profile with 20 axial zones is studied, but the choice of the case to be tested is left to the participants.
- It is recommended for all tasks to perform at least three calculation runs per case by using different starting random numbers. (Please, do not change the number of neutrons per generation in the calculation runs.)

### 3.2. Description of the test procedure recommended for testing convergence in the calculation of the fission density distributions

The test procedure recommended for testing convergence in the calculation of the axial fission density distributions is not the only possibly one that can be used, but it is a well-known and very simple procedure (cf. References /2/ and /3/) and is recommended, therefore.

Let  $N_{\text{skip}}$  denote the number of initial neutron generations skipped. To figure out the minimum number  $N_{\text{skip}}$  required for achieving convergence in the calculation of the axial fission density distribution it is necessary to perform a set of calculation runs with different numbers of initial generations skipped,

$$\left\{ (N_{\text{skip}})_k, k = 1, \dots, \kappa \right\}, \quad (N_{\text{skip}})_k \neq (N_{\text{skip}})_v \text{ for } k \neq v = 1, \dots, \kappa. \quad (3.2)$$

Without any loss of generality one may assume that

$$(N_{\text{skip}})_1 < (N_{\text{skip}})_2 < \dots < (N_{\text{skip}})_{\kappa-1} < (N_{\text{skip}})_\kappa. \quad (3.3)$$

Let  $n_k$  be the number of calculation runs performed with the  $k$ -th number of initial generations skipped,  $(N_{\text{skip}})_k$ ; and let  $(\text{SRN})_{kj}$  denote the starting random number used in the  $j$ -th calculation run performed with  $(N_{\text{skip}})_k$ ,  $j = 1, \dots, n_k$ .

It is a requirement of the test procedure described below that

$$(\text{SRN})_{kj} \neq (\text{SRN})_{v\mu} \text{ for all pairs } (k, j) \neq (v, \mu). \quad (3.4)$$

Let  $\rho_{ikj}$  be the fission density result obtained for the  $i$ -th axial zone in the  $j$ -th calculation run performed with  $(N_{\text{skip}})_k$  using the starting random number  $(\text{SRN})_{kj}$ ,

$$\rho_{ikj} \equiv \rho_i \left( (N_{\text{skip}})_k, (\text{SRN})_{kj} \right), \quad j = 1, \dots, n_k \text{ for } k = 1, \dots, \kappa; \quad i = 1, \dots, m. \quad (3.5)$$

Let  $\rho_{ik}$  denote the mean value of the observations  $\rho_{ikj}$  obtained for the  $i$ -th axial zone from the  $n_k$  calculation runs performed with  $(N_{\text{skip}})_k$ .  $\rho_{ik}$  is given by

$$\rho_{ik} = \sum_{j=1}^{n_k} h_{kj} \rho_{ikj}, \quad k = 1, \dots, \kappa; \quad i = 1, \dots, m \quad (3.6)$$

with

$$h_{kj} = \frac{(N_C)_{kj} - (N_{\text{skip}})_k}{\sum_{\mu=1}^{n_k} (N_C)_{k\mu} - (N_{\text{skip}})_k} \quad (3.7)$$

where  $(N_C)_{kj}$  denotes the total number of neutron generations calculated in the  $j$ -th calculation run performed with  $(N_{\text{skip}})_k$ .

$(N_C)_{kj}$  has to be chosen sufficiently large to avoid the observation of zero fission densities. It is therefore recommended to increase  $(N_C)_{kj}$ ,  $j = 1, \dots, n_k$ , when  $(N_{\text{skip}})_k$  is increased.

Note: If it is the case that for any axial zone  $\rho_{ikj} = 0$  is recorded in a calculation run, this run has to be restarted, i.e.  $(N_C)_{kj}$  has to be increased.

Provided that condition (3.4) is met the variance of the mean (3.6) is estimated by eq.(3.8),

$$s_{ik}^2 = \frac{1}{n_k - 1} \sum_{j=1}^{n_k} h_{kj} \cdot (\rho_{ikj} - \rho_{ik})^2, \quad k = 1, \dots, \kappa; \quad i = 1, \dots, m. \quad (3.8)$$

Provided that condition (3.4) is met the weighted mean of the mean values (3.6) obtained for the applied numbers  $(N_{\text{skip}})_k$ ,  $k = \kappa_{\min}, \dots, \kappa$ , is given by

$$\rho_i(\kappa_{\min}) = \frac{\sum_{k=\kappa_{\min}}^{\kappa} s_{ik}^{-2} \cdot \rho_{ik}}{\sum_{k=\kappa_{\min}}^{\kappa} s_{ik}^{-2}}, \quad i = 1, \dots, m, \quad (3.9)$$

where  $\kappa_{\min}$  denotes that value of  $k$  for which  $(N_{\text{skip}})_k$  is just the minimum required value of  $N_{\text{skip}}$ .

Due to the Central Limit theorem of Statistics (cf. Ref. /2/) the observations  $\rho_{ikj}$  for a given axial zone  $i$  can be taken as normally distributed. Then, due to linearity, the mean values (3.6) and the weighted mean (3.9) can also be taken as normally distributed. Therefore, the so-called “residual sum of squares” given by

$$Q_i^2(\kappa_{\min}) = \sum_{k=\kappa_{\min}}^{\kappa} \frac{(\rho_{ik} - \rho_i)^2}{s_{ik}^2}, \quad i = 1, \dots, m, \quad (3.10)$$

follows a  $\chi^2$ -distribution with  $(\kappa - \kappa_{\min})$  degrees of freedom (cf. Ref. /2/).

So,  $\kappa_{\min}$  is given by the lowest  $\kappa_{\min}$  value for which

$$Q_i^2 \leq \chi_{1-\alpha}^2 (\kappa - \kappa_{\min}) \quad (3.11)$$

is fulfilled for all  $k = \kappa_{\min}, \dots, \kappa$  and all  $i = 1, \dots, m$ .  $(N_{\text{skip}})_{\kappa_{\min}}$  is then, by definition, the minimum required value of  $N_{\text{skip}}$ .

$\chi_{1-\alpha}^2(\kappa - \kappa_{\min})$  denotes the  $(1 - \alpha)$ -point of the  $\chi^2$ -distribution with  $(\kappa - \kappa_{\min})$  degrees of freedom, and  $\alpha$  is the significance level of the test procedure (cf. Ref. /2/). Values for  $\chi_{1-\alpha}^2$  are given in Table 3.2.  $\alpha = 0.1\%$  is the usual choice for the test procedure described.

**Table 3.2: Values  $\chi_{1-\alpha}^2(\kappa - \kappa_{\min})$  of the  $(1 - \alpha)$ -point of the  $\chi^2$ -distribution with  $(\kappa - \kappa_{\min})$  degrees of freedom**

$(\kappa - \kappa_{\min})$	$\chi_{1-\alpha}^2(\kappa - \kappa_{\min})$					
	$\alpha = 10\%$	$\alpha = 5\%$	$\alpha = 2.5\%$	$\alpha = 1\%$	$\alpha = 0.5\%$	$\alpha = 0.1\%$
1	2.71	3.84	5.02	6.64	7.88	10.8
2	4.61	5.99	7.38	9.21	10.6	13.8
3	6.25	7.82	9.35	11.3	12.8	16.3
4	7.78	9.49	11.1	13.3	14.9	18.5
5	9.24	11.1	12.8	15.1	16.8	20.5
6	10.6	12.6	14.4	16.8	18.5	22.5
7	12.0	14.1	16.0	18.5	20.3	24.3
8	13.4	15.5	17.5	20.1	22.0	26.1
9	14.7	16.9	19.0	21.7	23.6	27.9
10	16.00	18.3	20.5	23.2	25.2	29.6
11	17.31	19.7	21.9	24.7	26.8	31.3
12	18.52	21.0	23.3	26.2	28.3	32.9
13	19.83	22.4	24.7	27.7	29.8	34.5
14	21.14	23.7	26.1	29.1	31.3	36.1
15	22.35	25.0	27.5	30.6	32.8	37.7
16	23.56	26.3	28.8	32.0	34.3	39.3
17	24.87	27.6	30.2	33.4	35.7	40.8
18	26.08	28.9	31.5	34.8	37.2	42.3
19	27.29	30.1	32.9	36.2	38.6	43.8
20	28.40	31.4	34.2	37.6	40.0	45.3
21	29.61	32.7	35.5	38.9	41.4	46.8
22	30.82	33.9	36.8	40.3	42.8	48.3
23	32.03	35.2	38.1	41.6	44.2	49.7
24	33.24	36.4	39.4	43.0	45.6	51.2
25	34.45	37.7	40.6	44.3	46.9	52.6
26	35.66	38.9	41.9	45.6	48.3	54.1
27	36.77	40.1	43.2	47.0	49.6	55.5
28	37.98	41.3	44.5	48.3	51.0	56.9
29	39.19	42.6	45.7	49.6	52.3	58.3
30	40.30	43.8	47.0	50.9	53.7	59.7

Check on Convergence of Fission Density Distribution

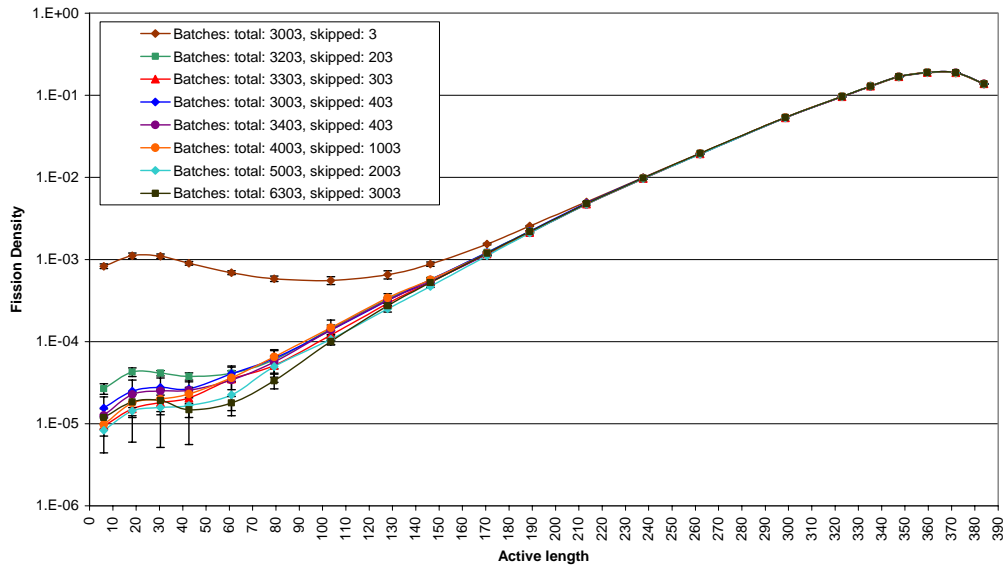


**Figure 3.1: Illustration of the test procedure described in section 3.2: Mean values (3.6) of the calculated axial fission densities and their one-standard confidence intervals (defined by  $\rho_{ik} \pm s_{ik}$ ,  $s_{ik}$  given by eq.(3.8)) for different numbers of initially neutron generations (batches) skipped**  
(Note: this example is taken from the Phase II-C report. In Phase II-E the active length is different.)

The test procedure described is a so-called “compatibility check” of the results  $\rho_{ik}$  (cf. Ref. /2/). The hypothesis under test,  $H_0$ , is:

- $H_0$ : All results  $\rho_{ik}$  represent observations from distributions with the same mean (and with correctly specified variances).

An alternative hypothesis  $H_1$  cannot be formulated since  $H_1$  is the set of all possible alternatives to  $H_0$ . It is a priori known that any alternative hypothesis leads to a better fit of the results than the weighted mean eq.(3.9) because  $H_1$  is sufficiently general to fit the data with any precision. It is therefore known in advance that  $H_1$  is better than  $H_0$  (from a purely statistical point of view). Since  $H_1$  cannot be formulated, the contamination (i.e. the probability of accepting  $H_0$  when it is false) is unknown.  $\alpha = 0.1\%$  is therefore the usual choice for the significance level (i.e. the probability of rejecting  $H_0$  when it is true) for test procedures like the one described.

So, in summary, the recipe for performing the test is as set forth below:

- Choose a first value  $(N_{\text{skip}})_1$  for the number of initial generations to be skipped and perform a set of  $n_1$  calculation runs using starting random numbers  $(\text{SRN})_{1j}$ ,  $j = 1, \dots, n_1$ . Note that condition (3.4) has to be met. Determine the mean value  $\rho_{i1}$  and the variance  $s_{i1}^2$  according to equations (3.6) and (3.8), respectively.

- Choose a second value  $(N_{\text{skip}})_2 > (N_{\text{skip}})_1$  for the number of initial generations to be skipped and perform a set of  $n_2$  calculation runs using starting random numbers  $(\text{SRN})_{2j}$ ,  $j = 1, \dots, n_2$ . Note that condition (3.4) has to be met. Determine the mean value  $\rho_{i2}$  and the variance  $s_{i2}^2$  according to equations (3.6) and (3.8), respectively.
- Continue with the procedure till you think that
  - convergence seems to be achieved and
  - the number  $\kappa$  of different  $N_{\text{skip}}$  values is sufficiently large for performing the test on convergence.<sup>2)</sup>
- Determine the weighted mean (3.9) and the residual sum of squares (3.10). When the acceptance criterion (3.11) is fulfilled for all axial zones  $i = 1, \dots, m$  then you have found the required  $\kappa_{\text{min}}$  and hence the minimum required number  $(N_{\text{skip}})_{\kappa_{\text{min}}}$  of initial generations to be skipped<sup>3)</sup>.

An example for applying the test procedure described is given in the EXCEL-file “**exemp\_conv\_check\_p2c.xls**” attached to this specification. (Note that this example was taken from the Phase II-C report.)

#### **4. Documentation of the calculation results**

An EXCEL-file named as “**p2e\_results\_name.xls**” is attached to this description. The calculation results shall be entered in this self-explanatory file. Columns for which no calculation results are available shall be left empty. Contributors to the benchmark are asked to replace the string “name” in the file name “p2e\_results\_name.xls” by a string adequate for identifying the contributor. (E.g., the author of this specification will rename the excel-file to “p2e\_results\_arevafanpgmbh.xls”.)

In addition to this excel file contributors to the benchmark are asked to provide a .doc-file or an ASCII-file which includes the following information:

- Institute / Company of the contributor
- Names of the participants
- Name of the computer code applied
- Name of the data library applied
- Brief description of computer code and data library.

---

<sup>2)</sup> For these purposes it is helpful to plot the mean values (3.6) together with their standard deviations (given by the square root of the variances (3.8)) as a function of the height of the fuel zones. Figure 3.1 shows an example (taken from the Phase II-C report).

<sup>3)</sup> If there are one or two axial zones for which the criterion (3.11) is not fulfilled (in contrast to all other axial zones) one may discuss whether or not  $\kappa_{\text{min}}$  is nevertheless acceptable. However, one needs good arguments for accepting  $\kappa_{\text{min}}$  in such a case.

Contributors to task No.3 and task No.4 are asked to give information about the outcome of the tests on convergence in the calculation of the fission density distributions. This information can also be entered in the EXCEL-file “p2e-results\_name.xls” (see fifth sheet in this file). However, *contributors who use a test procedure different from the one described in section 3.2, may generate their own adequate information sheet; and they are asked to give a brief description of the test procedure they have used.*

## 5. Planned evaluation of the results

From task No.1 and task No.2:

- End effect  $\Delta k$  as a function of the CR insertion depth
- Reactivity effect of the CR insertion on uniform burnup distributions and dependence of this effect on the CR insertion depth
- Looking for relations between these effects.

From task No.1 and task No.2:

- Characteristics of the axial fission density distribution as a function of the CR insertion depth for the uniform and non-uniform axial burnup profiles
- Looking for relations between these characteristics and the impact of the CR insertion on reactivity and end effect.

## 6. References

- /1/ Jens-Christian Neuber, “Generation of Bounding Axial Burnup Profiles as a Continuous Function of Average Burnup”, Proceedings of the Seventh International Conference on Nuclear Criticality Safety ICNC 2003, October 20 - 24, 2003, Tokai, Ibaraki, Japan, pp. 672 – 677
- /2/ Jens-Christian Neuber, “Remarks on  $k_{\text{eff}}$  calculation, fission density calculation and source convergence in criticality analysis using statistical codes”, AREVA, Framatome-ANP, August 11, 2005; paper prepared for the 14<sup>th</sup> meeting of the Expert group on Burnup Credit Criticality, London, August 26, 2005)
- /3/ W.T. Eadie, D. Drijard, F.E. James, M. Roos, B. Sadoulet, “Statistical Methods in Experimental Physics”, North-Holland Publishing Company, Amsterdam 1971